NASA CR-134,771
MDC-G5764

A TUNABLE LASER LINE FILTER POLYCHROMATOR FOR GAS TEMPERATURE MEASUREMENTS USING LASER RAMAN SCATTERING

by Jack J. Grossman and M. Muramoto

MCDONNELL DOUGLAS ASTRONAUTICS COMPANY-WEST

prepared for

NATIONAL AERONAUTICS AND SPACE ADMINISTRATION

NASA Lewis Research Center
Contract NAS 3-17818

1. Report No.	2. Government Accession No.	3. Recipient's Catalog No.
NASA CR-134,771		

4. Title and Subtitle	5. Report Date
A TUNABLE LASER LINE FILTER POLYCHROMATOR FOR GAS TEMPERATURE MEASUREMENTS USING LASER RAMAN SCATTERING	March, 1975
	6. Performing Organization Code
7. Author(s)	8. Performing Organization Report No.
J. J. Grossman and M. Muramoto	MDC-G5764
	10. Work Unit No.
9. Performing Organization Name and Address	11. Contract or Grant No.
McDonnell Douglas Astronautics Company-West 5301 Bolsa Avenue Huntington Beach, California 92647	NAS3-17818
	13. Type of Report and Period Covered
12. Sponsoring Agency Name and Address	Contractor Report
National Aeronautics and Space Administration Washington, D. C. 20546	14. Sponsoring Agency Code

15. Supplementary Notes

Project Manager, Jack A. Salzman, Physical Science Division, NASA Lewis Research Center, Cleveland, Ohio 44135

16. Abstract

A proprietary laser line filter spectrograph (LLFS) has been modified to test for improved remote measurement of atmospheric temperature by Raman spectroscopy of the rotational bands of N_2 and O_2. Both grating scan measurements with fixed PMT and polychromator image plane PMT scans with fixed grating setting were made using HeNe and Ar^+ lasers. The LLFS was found to have a laser line rejection ratio of 2×10^{12} at 6A from the laser line and provides resolved rotational Raman spectral display at the polychromator exit plane. Spectral resolution is adequate to measure and correct for background in the Stokes spectrum. It is anticipated that this system should allow measurement of gas or atmospheric temperature to ±1°C.

17. Key Words (Suggested by Author(s))		18. Distribution Statement
Laser	Raman Scattering	Unclassified - unlimited
Variable Wavelength	Gas	
Optical Filter	Temperature	
Polychromator	Lidar	

19. Security Classif. (of this report)	20. Security Classif. (of this page)	21. No. of Pages	22. Price*
Unclassified	Unclassified		$3.00

* For sale by the National Technical Information Service, Springfield, Virginia 22151

FOREWARD

We wish to acknowledge the technical assistance of M. B. Baker who designed and built the PMT polychromator image plane scanner, and Dr. J. A. Ryan for his help in all phases of the program.

Table of Contents

A TUNABLE LASER LINE FILTER POLYCHROMATOR FOR GAS TEMPERATURE MEASUREMENTS USING LASER RAMAN SCATTERING

by Jack J. Grossman and M. Muramoto

McDonnell Douglas Astronautics Company-West

Summary

A proprietary laser line filter spectrograph (LLFS) has been modified to test for improved remote measurement of atmospheric temperature by Raman spectroscopy of the rotational bands of N_2 and O_2. Both grating scan measurements with fixed PMT and polychromator image plane PMT scans with fixed grating setting were made using HeNe and Ar^+ lasers. The LLFS was found to have a laser line rejection ratio of 2×10^{12} at .6 nm from the laser line and provides resolved rotational Raman spectral display at the polychromator exit plane. Spectral resolution is adequate to measure and correct for background in the Stokes spectrum. It is anticipated that this system should allow measurement of gas or atmospheric temperature to ±1°C.

Introduction

Rotational Raman lidar is a technique having potential for the remote measurement of air/gas temperature (cf. References 1-5). A major problem has been the achievement of desired sensitivity and accuracy due to aerosol fluorescence and laser line interference with the rotational Raman lines, which lie close to the laser line. One objective of this program has been to determine the ability of a modified MDAC laser line filter spectrograph (LLFS) system (Reference 6) to reject laser line intensities so that the multiline information contained in a complete rotational spectrum of air can be time resolved in parallel. Another objective has been to determine whether the LLFS system coupled with suitable input optics can improve remote air temperature measurement accuracy by directly measuring and subtracting the fluoroscence background from the Raman line intensities.

In order to accomplish these objectives the following approach was utilized:

- Design, fabricate and test a modified laser filter mirror assembly for measuring the rotational Stokes and anti-Stokes Raman lines. Also, design, fabricate and test a polychromator plane scanning slit and photomultiplier assembly. Design goals included an attenuation factor of 10^{-10} for the laser line intensity within 20 wave numbers on either side of the laser line frequency.
- Measure the rejection efficiency and overall system throughput for the laser line filter spectrograph. Included in this was detailed measurement of spectral line shapes at several mirror slit widths and exit slit aperture widths.
- Recommend a specific instrumental configuration for field application of the system in the NASA-Lewis Research Center Raman Lidar Unit.

The objectives have been successfully accomplished and a system has been defined which should remove the above-noted problems (fluoroscence and laser line interference). It is anticipated that this system should allow measurement of gas or atmospheric temperature to at least ±1°C.

Laser Line Filter Spectrograph (LLFS) Description

The MDAC laser line filter (LLF) is shown schematically in Figure 1. Briefly light entering the spectrometer slit is dispersed by the grating and an MDAC proprietary design mirror placed at the spectral image plane. The grating can be rotated so that the laser line either exits the mirror slit or is moved onto the mirror and reflected back. This can also be accomplished by keeping the grating fixed and translating the mirror along the image plane so that the laser line again either exits the slit or is reflected back. All rays, which are reflected back from the spectral plane, reform at the exit aperture. In other words the filter acts as a zero order double spectrograph. If the laser line is reflected back the laser line intensity at the exit aperture is called unity. If the laser line exits the filter mirror slit, the laser line intensity at the exit aperture should be about 10^{-7} of the reflected intensity.

The prototype laser line filter system (Figure 2) was built by modifying a standard Jarrell-Ash 25-104 (Figure 3) 3/4 meter double monochromator. This

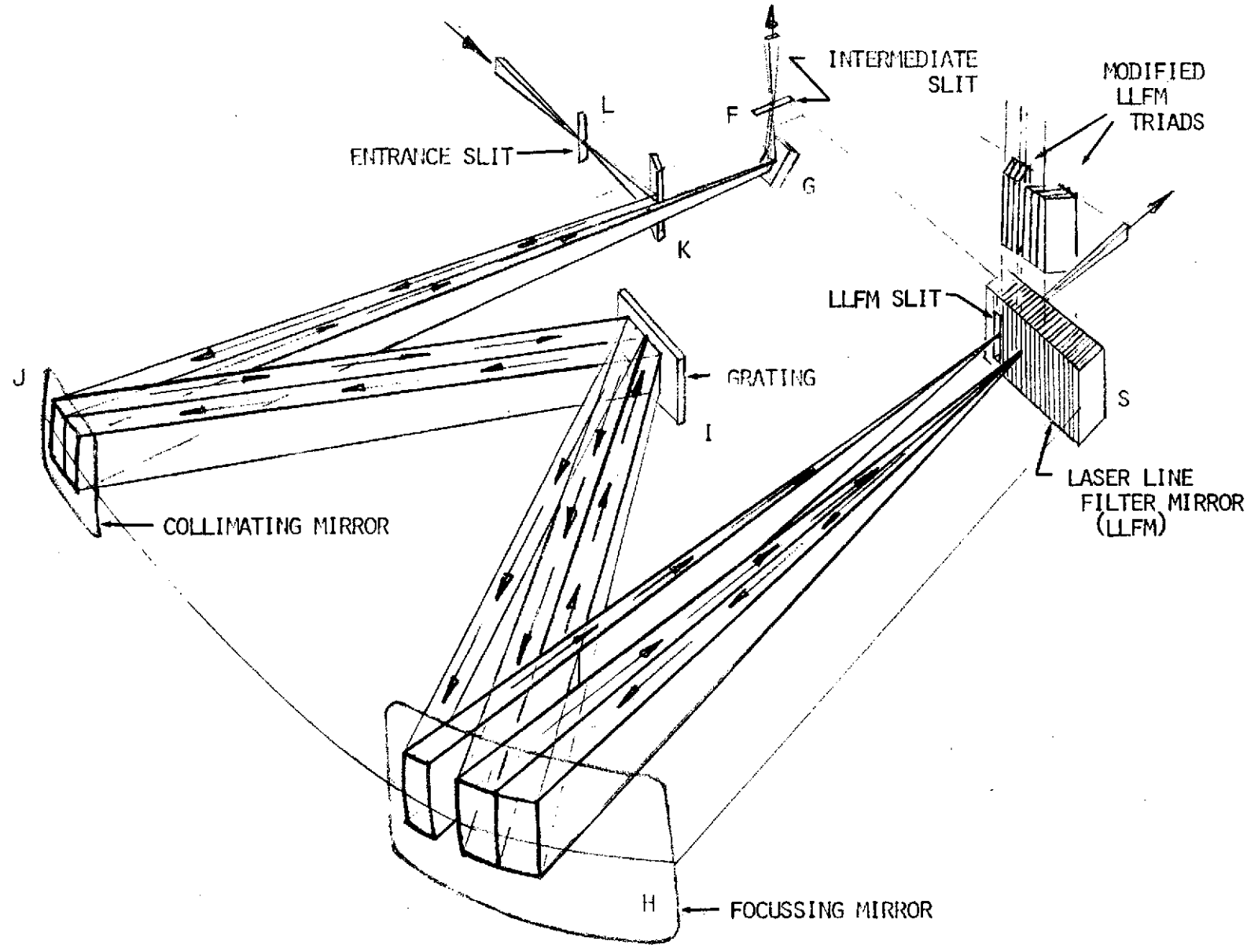

FIGURE 1. Schematic Diagram of Central Ray Bundle Paths for Two Wavelengths in MDAC-West Laser Line Filter

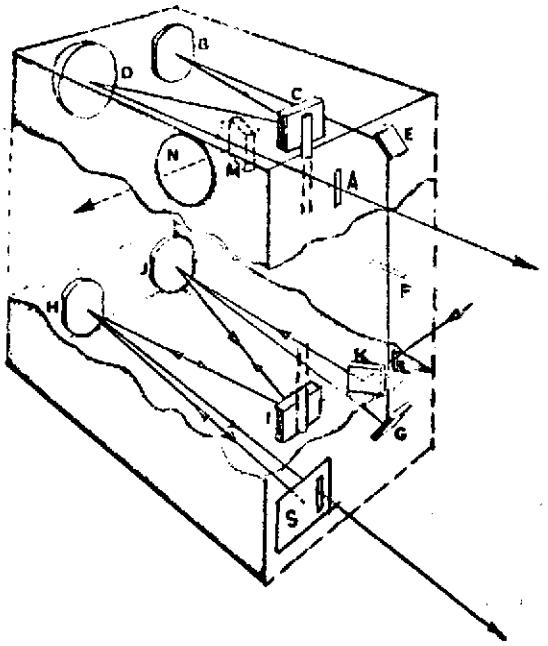

OPTICAL LAYOUT: LASER LINE FILTER SPECTROGRAPH

L. entrance slit
K. 45° mirror
J. collimating mirror
I. grating
H. focussing mirror
S. laser line filter mirror and filter slit
S.H.I.J.G. return path of filtered light
G. 45° mirror
F. intermediate slit
E. 45° mirror
B. collimating mirror
C. grating
D. camera mirror
M. 45° mirror
N. polychromator output plane
A. monochromator output slit

FIGURE 2. LAYOUT OF LASER LINE FILTER SPECTROGRAPH (LLFS)

Optical Layout 25—100
Double monochromator

A. entrance slit
B. collimating mirror
C. grating
D. camera mirror
E. 45° mirror
F. intermediate slit
G. 45° mirror
H. collimating mirror
I. grating
J. focusing mirror
K. 45° mirror
L. exit slit
M. swing out mirror
N. light path when using only upper section

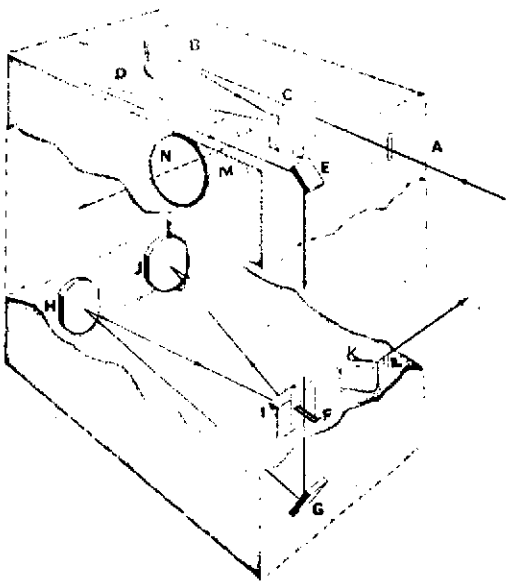

FIGURE 3. OPTICAL LAYOUT JARRELL-ASH 25-104 3/4 METER DOUBLE MONOCHROMATOR

included (Figure 2): (a) Interchanging the entrance slit and intermediate aperture assembly, E, F, and G; (b) replacing the lower collimating mirror H with a larger mirror to make both the lower and upper mirror systems; (c) placing the MDAC filter mirror (LLFM) so that the slit in the mirror(s) is directly under the slit A; (d) replacing the diagonal mirror for the slit K with a half mirror (see Figure 1); and (e) reversing all slits so that the light travels from L to F to A for a single spectral line or from L to F to the refelcting mirror M forming the complete spectrum in polychromator housing N. Direct calibration of the spectrograph filter attenuation at the exit slit or at the polychromator image plane was accomplished using variable slit widths and the wide dynamic range of the photomultiplier tube to calibrate the total system throughput. Indirect calibration was accomplished also by using filters of known attenuation.

Two noise sources which limit rotational Raman temperature measurement accuracy in the LLFS are the natural laser line wing shape produced by imperfect diffraction interference from a grating with finite dimensions, and light scattered randomly into the spectrograph through the intermediate slit. The diffracted line shape produced by a perfect grating and a laser line (λ) with bandwidth $\Delta\lambda_n$ is essentially the doppler, pressure broadened natural line width. With a real grating the observed bandwidth $\Delta\lambda$ is greater than the natural bandwidth because the finite number of diffraction lines produces imperfect interference hence wings in the diffraction pattern. Jarrell-Ash gratings (used in this program) have wings which are 4.5 orders of magnitude or more down from the peak laser light intensity when $\Delta\lambda \geq 0.5$ nm. Randomly scattered laser light noise from the components of the filter spectrometer is eliminated by means of the laser line filter (Figure 1).

The direct beam laser light exits the filter section through the LLFM slit into a black compartment. Only a small fraction of this backscattered light reenters the filter compartment. This small fraction appears to come from a real slit source at the proper position for the grating to refocus it at the intermediate slit. The only additional source of laser light is from the laser line diffraction wings reflected back from the LLFM. Theoretically this wing light intensity at the intermediate slit (F) should be down by seven orders of magnitude 10^{-7} from the light intensity incident on the entrance slit.

The LLFM was originally built for vibration Raman line measurements and thus covered a 3600 cm^{-1} band spread. However, for rotational Stokes and anti-Stokes measurements only 300 cm^{-1} on either side of the Rayleigh line is required. Additional noise reduction is possible therefore by limiting the filter mirror spectral bandwidth to ± 300 cm^{-1}, thereby reducing the back reflected laser line wing light by a factor of six.

The LLFM produces minimum aberration, hence best resolution, when close to the minimum distance between the virtual entrance slit and the exit slit of the Czerny-Turner mounting. To maintain best resolution and obtain the anti-Stokes rotational Raman spectrum the mirror slot was moved 300 cm^{-1} towards longer wavelengths, Figure 1. To minimize noise, the Stokes Raman side was also limited to 300 cm^{-1} bandwidth as explained above. The laser line filter assembly is shown in Figure 4.

A capability is required for PMT scanning of the polychromator spectral plane since PMT, rather than photographic, detection is needed to simulate lidar temperature measurements. The photomultiplier tube used was the Hamamatsu R212. The preferred low noise end window PMT was too large to use without a major redesign and fabrication effort. Instead, the standard side window PMT housing mounted on a precision Gaertner micrometer transport assembly was used. This was sufficiently compact to be enclosed in the standard Jarrell-Ash polychromater housing. The micrometer screw was coupled to a variable speed reversible gear drive train through a light tight bushing. The completed scanning system is shown in Figure 5.

Experimental Procedures and Measurements

Laser Line Filter Mirror (LLFM) Fabrication

A six segment mirror (Figures 1 and 4) was designed to duplicate the angles and orientation of segments #2 through #7 of the existing MDAC laser line filter mirror. This limited the spectral bandwidth to 300 cm^{-1} on either side of the LFM slit. The modified MDAC mirror was then mounted in a specially constructed assembly and test jig, and the mirror angles measured using a HeNe laser for a light source with a ten meter optical lever. The spot positions were marked on graph paper attached to a wall at one end of the ten meter optical lever.

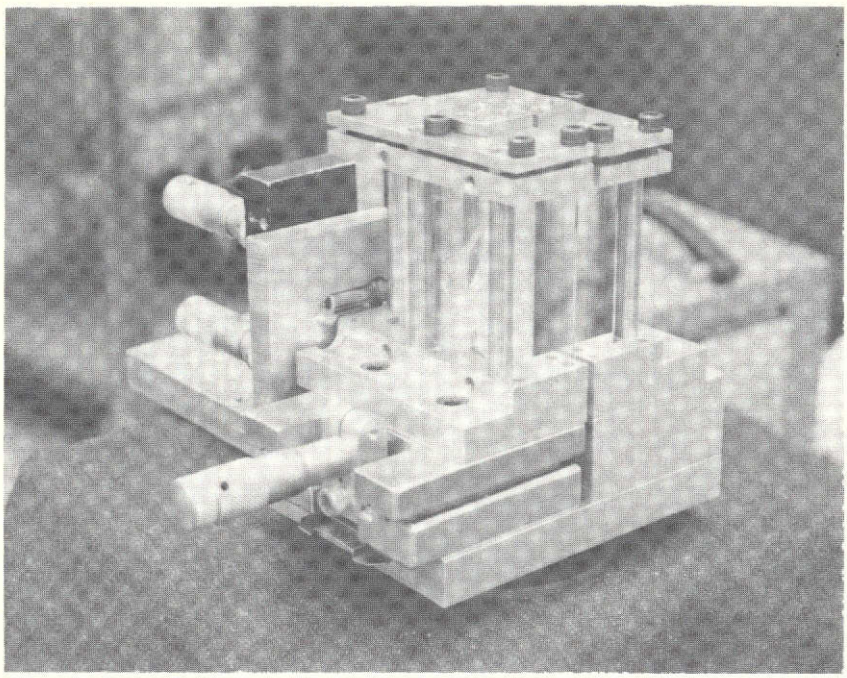

FIGURE 4. LASER LINE FILTER MIRROR (LLFM) ASSEMBLY

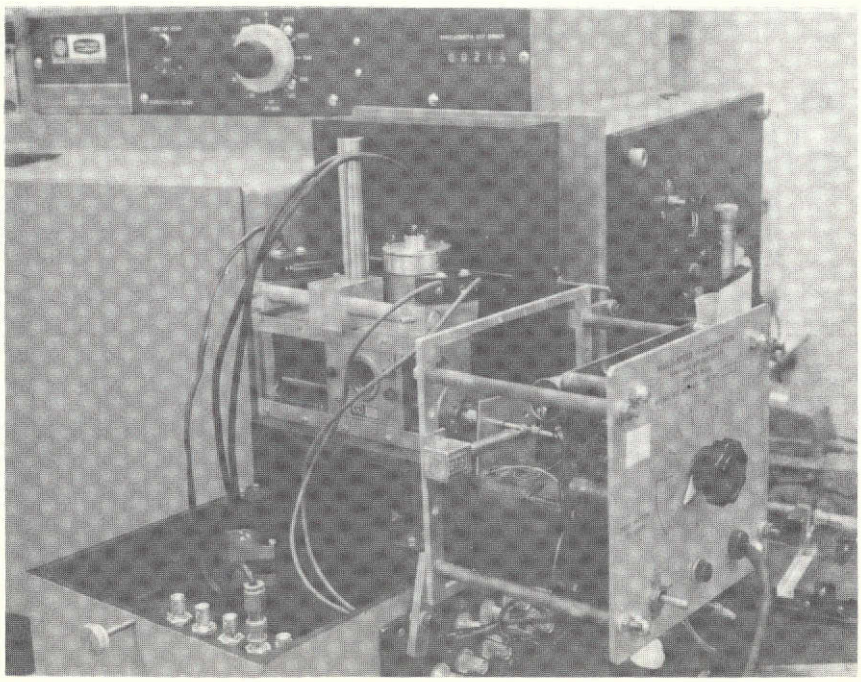

FIGURE 5. MICROMETER DRIVE ASSEMBLY FOR POLYCHROMATOR PLANE PMT/SLIT SCANNING

The MDAC mirror was then removed and glass plates stepwise inserted into the same assembly and test jig to form two triads. Each plate was adjusted until the laser spot was superimposed on the recorded spot from the corresponding plate of the MDAC mirror. After alignment of each mirror triad, the triad plates were bonded with water glass and epoxy and the alignment rechecked to ensure that no distortions had been introduced during resin curing. A mount for the modified laser filter mirror (triad pair with variable slit width between) was then designed and fabricated. Prior to mounting the cemented triads, the polished mirror faces were vacuum coated with aluminum. Finally, scattered-light baffles were mounted between the laser filter mirror and the spectrograph face plate to minimize laser light (transmitted through the LLFM aperture) reentering the filter section of the spectrograph.

Modified Entrance Aperture Mirror Assembly

During tests for stray light decoupling between the two spectrograph compartments (Figure 2) we found that illumination of the grating I by light from the entrance slit L which missed the top of the first mirror K caused excessive scattered light to pass the intermediate slit F. Attempts to realign the spectrograph further convinced us that time could be saved by replacing the entrance mirror assembly K with one designed for easier access to adjusting and aligning screws. Therefore a new mirror assembly was designed and fabricated.

Polychromator Plane Scanning Slit and Photomultiplier Assembly

This mechanism (Figure 5) mounts at the exit aperture of the Jarrell-Ash spectrometer and comprises a motor-driven linear motion device to which is attached a photomultiplier and slit. It was designed around an existing Gaertner scanning microscope mount and the Jarrell-Ash polychromator housing. The required mounts were fabricated out of aluminum, optically blackened, and a photomultiplier housing attached to the scanning microscope linear motion mechanism. The device was then mounted in the housing in such a manner that the existing polychromator exit slit could be coupled to the photomultiplier housing and both could scan across the Jarrell-Ash exit aperture. A variable speed reversible electric motor drive train was attached to the linear motion screw by means

of a shaft through the housing cover. Finally, limit switches and a revolution counter (for slit position) were installed.

Grating and PMT Scanning

Each point N on the polychromator image plane N (Figures 1, 2 and 6) has a corresponding spectral point S_i in the LLFM plane S. If the grating dial setting is λ_L when the laser line initially exits the LLFM slit S_L, then every other point on the LLFM $S_{\Delta\lambda}$ and polychromator image plane $N_{\Delta\lambda}$ has a corresponding wavelength $\lambda_L \pm \Delta\lambda$, which depends only on the grating dispersion (1.1 nm $(mm)^{-1}$ in this work). When the grating is fixed at dial setting λ_L (Figure 6A) the transmitted spectrum (less the laser line exiting the LLFM slit) may be scanned by driving the PMT detector across the polychromator focal plane N. If on the other hand, the mirror M is rotated or translated all points in the LLFM plane are translated and rotated in the polychromator exit plane. Alternatively, translation of the LLFM aperture in the LLFM plane causes a corresponding translation of its image in the image plane N and a relative change in the PMT position reading. Finally, translating the laser line into the new slit position translates all wavelengths a corresponding amount in the LLFM plane and the polychromator plane.

The main characteristics of the grating scan are shown in Figures 6A and 6B in which corresponding Figure 2 component part designations X used for the LLF section are placed in parenthesis (X) and those for the upper polychromator section are given without parenthesis X.

Figure 6A shows the paths of three spectral rays, a Stokes line $(\lambda_{s'})$, an anti-Stokes line (λ_{as}) and the laser line (λ_L) where the laser line is exiting the LLFM slit and the PMT detector P is set to measure the Stokes line $\lambda_{s'}$. The grating setting for this case is called $C(\lambda_L;\lambda_{s'})$. By rotating the grating toward shorter wavelengths through an angle corresponding to $(\lambda_L - \lambda_{s'})$, the configuration shown in Figure 6B is obtained, where the grating setting is $C(\lambda_{as};\lambda_L)$. In this case the anti-Stokes line λ_{as} exits the LLFM aperture and the laser line falls on the detector.

As the grating rotates the spectrum translates along both the LLFM and the polychromator image planes. The maximum PMT signal for the laser light occurs when the grating dial wavelength reading corresponds to the wavelength of light seen by the PMT when the laser wavelength is exiting the LLFM aperture.

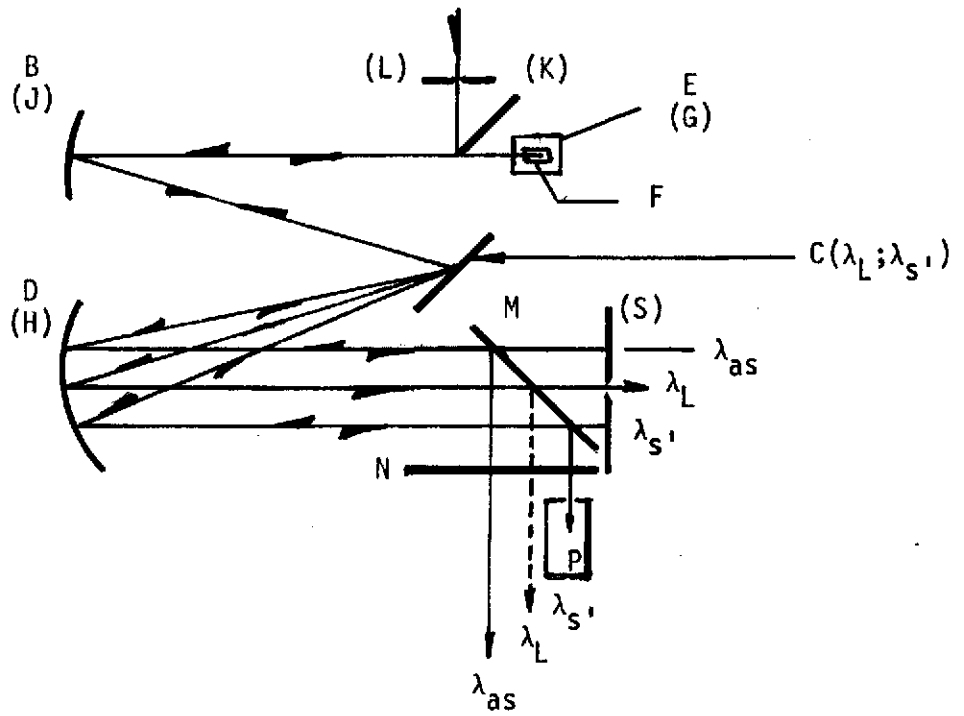

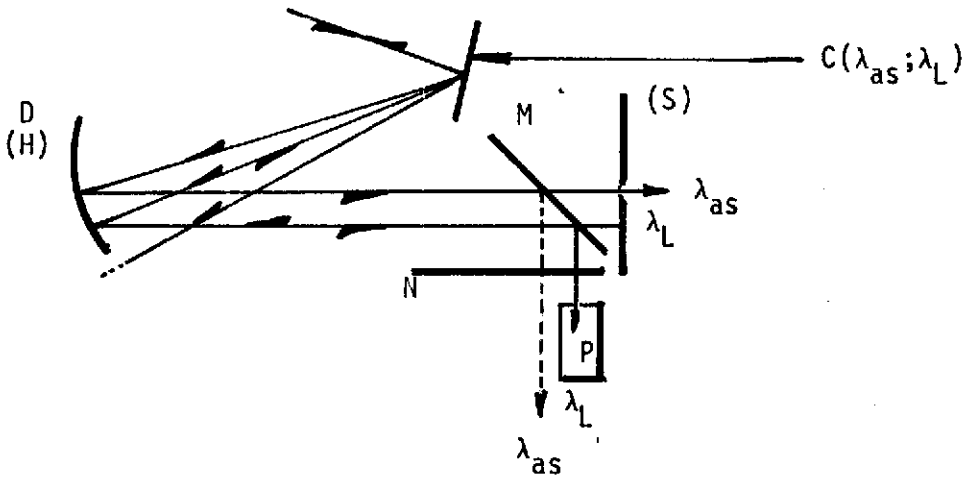

FIGURE 6. Central Ray Paths for Three Wavelengths With Fixed PMT Detector and Two Grating Settings A and B

An example is shown in Figure 7. The laser line starts at the spectral position corresponding to the wavelength 619 nm where the PMT signal is found to be 1.8×10^{-9} amps. As the wavelength drive rotates, the laser line moves closer to the PMT tube and the signal increases slowly to 3.5×10^{-8} amps. If the LLFM aperture were not present the PMT signal would continue to increase along the dotted line. However, as the line enters the LLFM aperture (slit), the laser line is removed from the system instead of being reflected and the intensity decreases to a value equal to or less than the PMT noise background. The signal stays at background until the laser line starts reflecting from the other edge of the LLFM aperture. It then continues to rise and reaches a maximum when the central laser line rays enter the PMT aperture. The signal then decreases as shown until it passes the other end of the mirror.

Rejection Efficiency

The laser line rejection efficiency $\rho(L)$ is defined as

$$\rho(L) = \frac{I(\lambda_L;\lambda_L)}{I(\lambda_L;\lambda)}$$

where $I(\lambda_L;\lambda)$ is the laser light intensity at λ_L when the system is set to measure light intensity at the wavelength λ, and $I(\lambda_L;\lambda_L)$ is the laser light intensity at λ_L when the system is set to measure light intensity at the laser wavelength λ_L. Its reciprocal $\tau(L)$ is denoted as the attenuation ratio or the transmission efficiency. If $I(\lambda;\lambda)$ is the signal intensity at wavelength λ when the system is set to measure the signal at wavelength λ, then the signal to laser line noise is

$$\frac{S}{N} = \frac{I(\lambda;\lambda)}{I(\lambda_L;\lambda)} = \frac{\rho(L)\ I\ (\lambda;\lambda)}{I(\lambda_L;\lambda_L)}$$

The rejection efficiency can be found by measuring both the laser line shape and then the peak laser line intensity when the filter is used. An example using a wavelength scan is shown in Figure 7. It was made by setting the PMT slit (500 μm wide) at the polychromator image plane position corresponding to one edge of the LLFM aperture and then rotating the grating. The

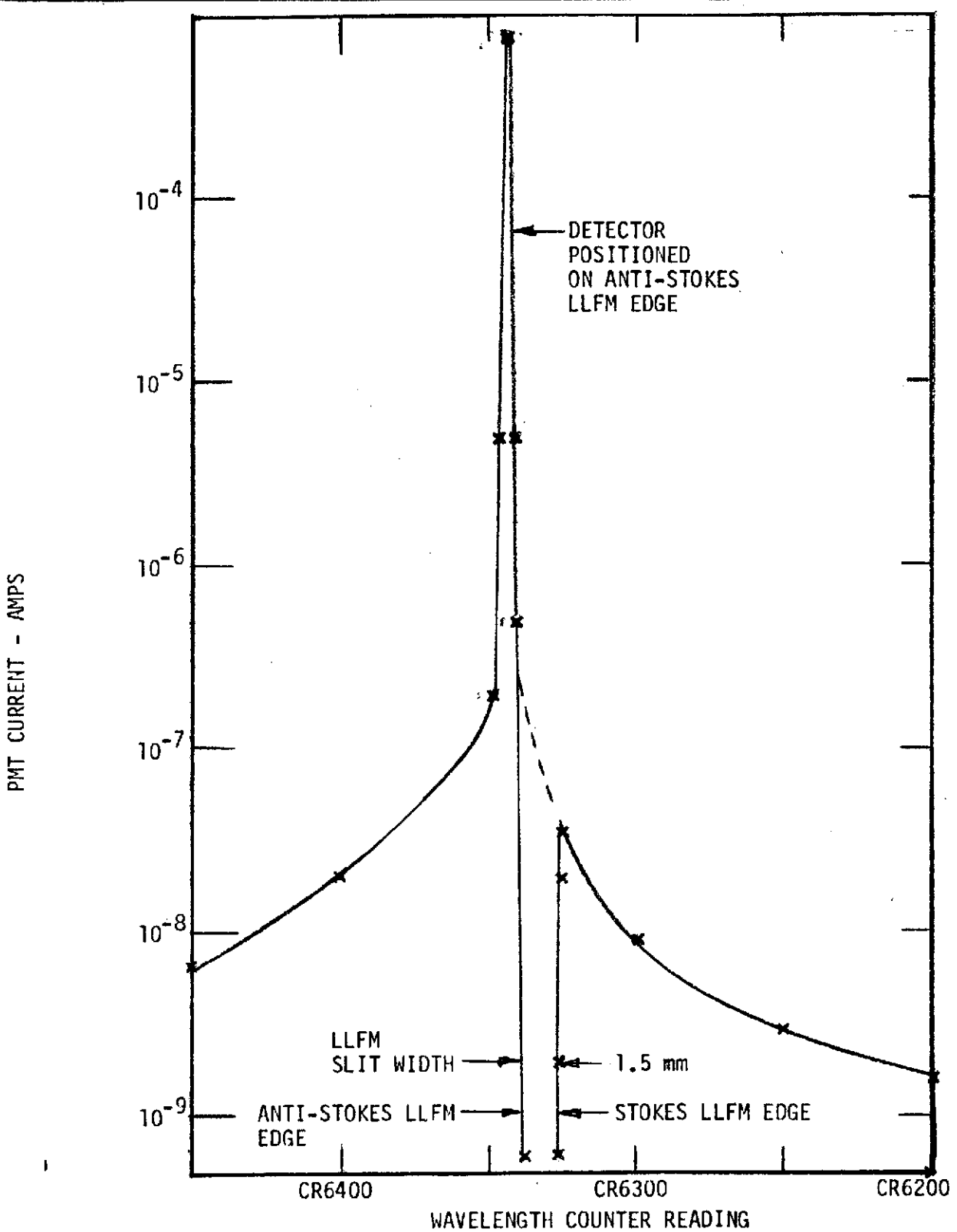

FIGURE 7. Grating Scan with HeNe Laser 632.8 nm Entrance, Intermediate and Exit Slits Were Each 500 μm Wide.

laser beam was focused on a compacted powdered Lambertian $BaSO_4$ target and the scattered light was imaged on the entrance slit with an F1.2 lens. The entrance, intermediate and PMT slits were each 500 μm wide. Although the basic Jarrell-Ash spectrograph optics are F7, the modified system, Figure 1, makes use of only half the mirror and grating for rays going to the LLFM and the other halves for the rays reflected back to the intermediate slit. Therefore a theoretical gain in intensity by a factor of two is possible.

Experimental Results and Discussion of Results

Rejection Efficiency with HeNe Laser

The modified laser filter system was found to meet the design specification goal namely: an attenuation of the laser line frequency greater than 10^{-10} within 20 cm^{-1} on either side of the laser line frequency. These measurements are summarized in Figure 8, again for HeNe, wherein the logarithm of the PMT current (left ordinate scale) is plotted as a function of the detector position X (upper abscissa scale) scanning the spectrograph image plane for six different settings of the grating counter (lower abscissa scale). The complete spectrum is shown for the grating counter reading CR6320. Here the laser line falls on the LLFM surface and the spectrum which is measured by the PMT scan is the reference signal, equivalent to a Raman line centered at 34.2 mm. Far from the line center at 31.3 mm ($\Delta\lambda$ = 30Å) the transmitted intensity of the wings of the laser line is down 10^{-5} from the intensity at the line center. At a displacement of 20 cm^{-1} from the laser line the intensity is $10^{-4.5}$.

Similar spectral plane PMT scans were made at the grating settings CR6320, CR6324, CR6326, CR6328, CR6348, and CR6350. These are shown as the points Δ in Figure 8. The connecting line is the maximum signal intensity which would be observed at any setting CRxxxx. Five additional partial spectra are shown, limited to about .25 nm from the midpoint of the laser line. PMT noise current was measured to be about 10^{-10} amps and it is shown as a baseline in the LLFM slot.

When the grating counter reading is increased from CR6324 to CR6330, the laser line enters the LLFM slit and a dramatic decrease is observed in the maximum transmitted intensity. A proportional decrease is observed in the wings. There is an indication that the wing transmission ratio is asymmetrical,

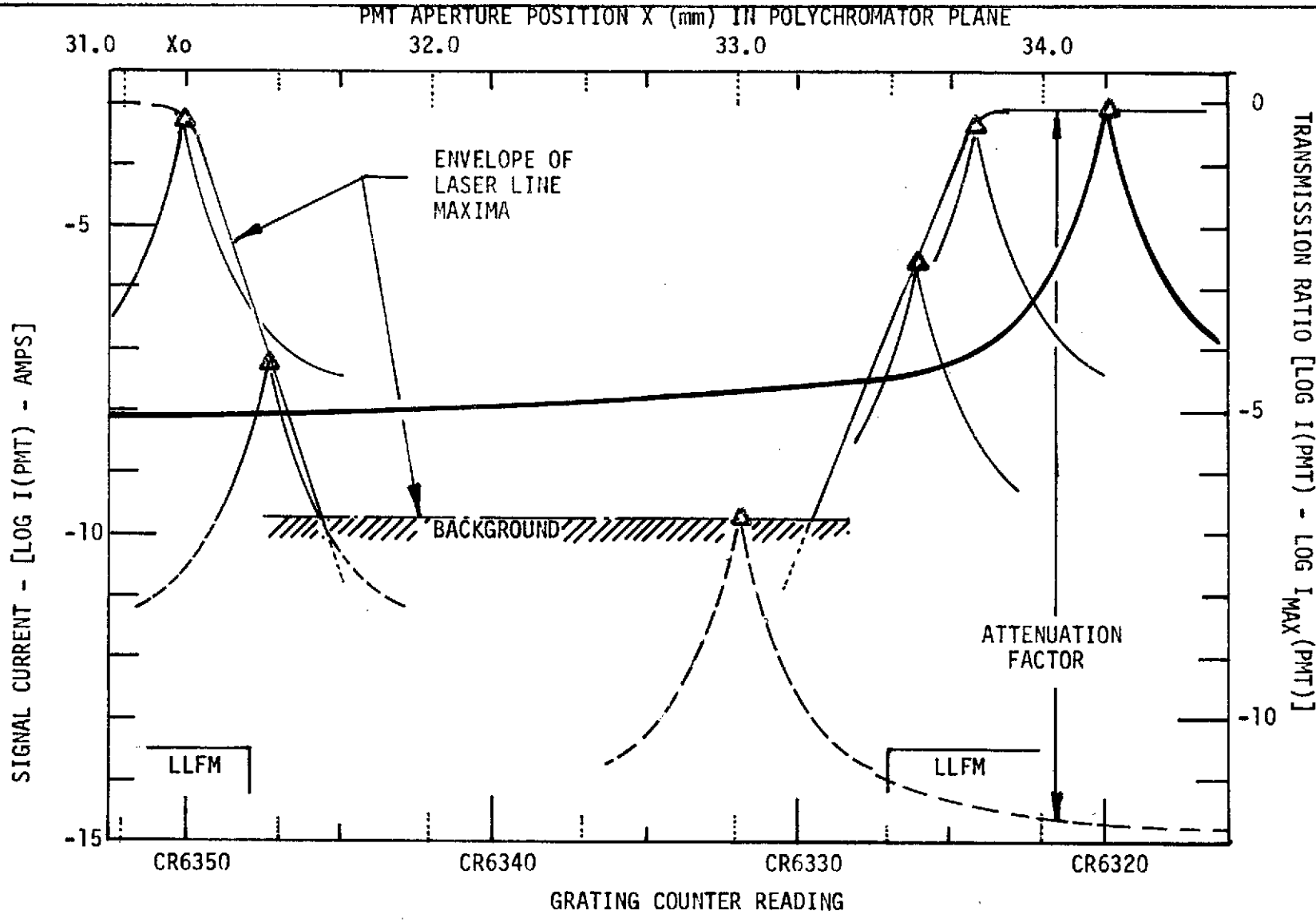

FIGURE 8. Photomultiplier Tube Spectral Plane Scans of the HeNe 632.8 nm Laser for Six Grating Counter-Readings. The Laser Line is Near to or Exiting the LLFM Slit.

namely, the side on the LLFM slot falls to a lower value than the 10^{-5} value observed for reflection off the front mirror surface at positions $31.3 > X > 33.8$. This could be caused by multiple scattering of laser light through the front surface of the LLFM aluminum coating.

Since the minimum detectable signal is 10^{-10} amps, and no signal is observed when the laser line is exiting the LLFM slot ($31.9 < X < 33.1$), the maximum possible laser line signal is 10^{-10} amps. Since the wings of the laser line also have the same shape when measurable on the downslopes of the envelope curve, the maximum possible wing signal follows the characteristic shape of grating diffraction pattern, shown as the dashed curve centered at CR6332.

In Figure 8, the smallest separation of λ_L and λ occurs when the laser line is centered at 33.2 and the Raman line is at 33.8 ($\Delta\lambda$ = 0.66 nm). That is, when the laser line is in the LLFM slit at grating setting CR6346 and the PMT slit is positioned at 33.8 equivalent to CR6350. The PMT signal is the sum of the Raman line at 633.4 nm and residual laser line signal 6Å from the laser line at 632.8 nm. Consequently, from Figure 8, the attenuation ratio is found to be $10^{-11.25}$ and the rejection efficiency $\rho(L) = 1.75 \times 10^{11}$. This is a factor of 17.5 better than the design specification goal.

With the 500 μm PMT slit width used the spectral resolution was 0.6 nm which is equal to the observed $\Delta\lambda_{min}$ at CR6330, the minimum separation between the center of the laser line and the Raman line with the rejection ratio $\rho(L) \geq 10^{11.25}$. If the spectral resolution of the system is less than 0.6 nm, then the minimum separation between the rotational Raman lines and the laser line can be decreased by narrowing down both the intermediate and exit apertures to match the LLFS system resolution.

Measurements With Argon Ion Laser

A second series of tests was performed using an Argon ion laser with a power increase of 100 over the HeNe laser. Figure 9 shows a series of polychromator plane PMT detector scans at different settings of the grating using the green 514.5 nm line. The laser beam power was approximately 500 mW, the entrance, intermediate and PMT slits were all 500 μm wide, and the LLFM slit was 1.5 mm. Complex line shapes are produced when the laser beam partly enters the slot and is scattered off the edge, CR5130.

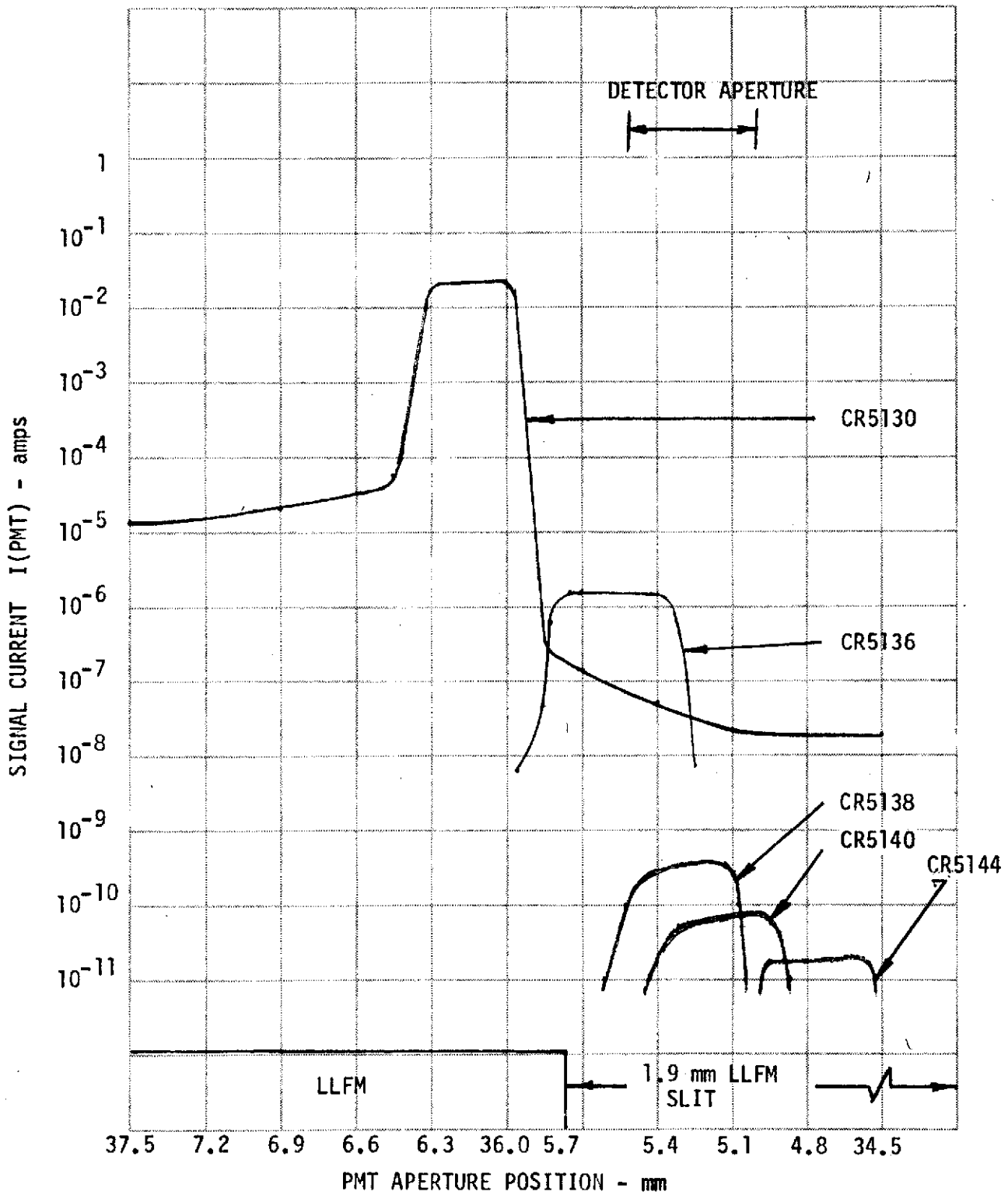

FIGURE 9. PMT/Slit Scan of Polychromator Output Plane at Five Grating Drive Counter Readings (λ_L = 514.5 nm).

As the laser line enters the LLFM slit, the peak intensity (514.5 nm) decreases to a minimum of 2×10^{-11} amp. The light backscattered from the slit (CR5144) is a factor of 2 over the tube background noise. Using the high powered Ar^+ laser the PMT anode voltage must be decreased to prevent tube saturation effects. This lower voltage explains the decreased noise level in these measurements compared with the HeNe values, Figure 7. No attempt was made to limit this backscattered signal by decreasing the slot width or using matte black, light absorbing paint. The peak input signal was measured to be 2.65×10^{-5} amps with neutral density filters (nd=3 used at the input to prevent saturating the PMT). The peak laser input signal is therefore 2.65×10^{-2} amps and the total attenuation of the laser line is 8×10^{-10}. This is two orders of magnitude better than expected. Since the wings of this LLFM aperture are a factor of 10^{-4} down from the filter peak at 6Å away, the net attenuation of the laser line at the nearest Raman line could be as low as 10^{-13}. Again this assumes that the observed PMT noise is the limiting noise current.

LLFS System Throughput

Measurement of the LLFS system transmission efficiency was made using the monochromatic 514.5 nm laser line. When all the data were taken by PMT scanning of the spectral plane, analysis showed that the exit plane slit did not remain fixed. A small unpredictable slit rotation was found with respect to the intermediate slit which always led to low, nonreproducible system throughput values. (This problem didn't effect the rejection efficiency measurements except to show they are worst case minimum values and could be improved.) In place of these, grating scan measurements were made using a fixed slit optically aligned with the intermediate slit. The slit was placed well away from the LLFM slit so that no slit edge effect could lower the throughput energy especially of the rotational Raman line nearest the LLFM slit.

The light source was the 5145Å laser line scattered off a standard $BaSO_4$ diffuse reflector. The input signal was measured using the same photomultiplier tube held in a PMT tube housing at the same distance from another aperture/shutter which duplicated the LLFM entrance slit geometry. We found that the slit micrometer calibrations were not accurate and variations were found in the energy density (the ratio of the measured energy divided by the slit width).

The experimental results are summarized in Table 1. The data for the 80 μm and 200 μm are the most reliable. (Sufficient time was not left to calibrate the LLFS entrance and intermediate slits accurately in time for this report.)

In Table 1, LLFS calibration data are given above the entrance slit calibration data. The measured PMT current is given in the last line as a function of the slit width shown at the top of the table. LLFS slit widths are tabulated in the first three columns. The peak current in μ amps are given in the fourth column. The percentage transmission is calculated using the LLFS signal given by row and calibration signal at the bottom of the appropriate column. Finally, spectral peak half widths are given in the last column.

The average value of the 80 μm and 200 μm data is 8.8%. This number should be multiplied by a factor of 2 since half the energy is lost by masking (only half the grating is used) and the transmission is found to be about 18%. This value is in good agreement with the calculated system efficiency: 96% reflection efficiency from each of 11 mirror surfaces and 65% grating efficiency from each of 3 grating reflections to give an 18% total throughput. This compares favorably to dielectric filter transmissions which range from 10% to 40% when the stop band transmission is below .01%. The factor of 2 in signal for the better dielectric filters is compensated in the LLFS system by the increased energy gained from using the additional rotation transitions close to the laser line.

The experimental results reported in this section show that the LLFS system is significantly better than expected. Since a laser line attenuation of 10^{-12} is found, remote atmospheric temperature measurement is possible even in highly turbid conditions until signal attenuation due to Mie scattering itself limits the backscattered signal. Additional gain in signal can be obtained by AR coating all optical components. The expected reflectivity is then 99% and the 11 mirror surfaces would have a transmission of 89.5%, or a gain of 40% over uncoated optics. As shown in Appendix A, this improvement in signal bandwidth and spectral resolution implies an ability to measure air temperatures to better than ±1°C, an improvement of 4 over Salzman and Coney's dielectric filter measurements (References 1 and 2).

TABLE 1

LASER LINE FILTER SYSTEM
LIGHT TRANSMISSION EFFICIENCY

SLIT WIDTH SETTINGS μm			PEAK CURRENT	% TRANSMISSION SMALLEST SLIT				PEAK HALF WIDTH
ENTR.	INT.	EXIT	μ AMPS	500	200	80	20	
500	500	500	0.53	5.9%				6.3Å
500	200	500	0.27		8.2%			5.1Å
500	80	500	0.123			9.0%		5.0Å
500	20	500	0.020				12.6%	6.0Å
500	500	200	0.28		8.5%			4.8Å
500	200	200	0.26		8.7%			2.3Å
500	80	200	0.13			9.6%		2.2Å
500	20	200	0.022				13.8%	1.8Å
ENTRANCE SLIT CALIBRATION CURRENT μ AMPS				9.9	3.4	1.28	.16	

Conclusions

The objectives of this program were to determine the ability of a modified LLFS system to reject laser line intensities so that multiline Raman spectra can be time resolved in parallel, to measure the total system throughput, and to determine whether the LLFS system coupled with suitable input and output optics can improve air temperature measurement accuracy. A modified laser LLFM to transmit both Stokes and anti-Stokes rotational Raman lines and a polychromator plane PMT scanning assembly were designed and fabricated.

Measurements were made to determine the system characteristics. All design objectives were met. The results were (1) the relative laser line rejection at the peak of the first rotational Raman line ($\Delta\lambda$ = 20 cm^{-1}) was 10^{11},(2) if internally scattered laser light is not the limiting noise current, then the rejection ratio is probably near 10^{12} and could be increased to 10^{13}, (3) light throughput was measured to be 9%, (4) the throughput could be increased by a factor of 2 with modified input optics and by another factor of 1.4 using AR coated optics, (5) these throughput values are comparable to or better than multilayer dielectric filter throughput values, and (6) atmospheric temperature measurements could be made to better than ±1°C.

References

1. Salzman, J. A.; and Coney, T. A.: Atmospheric Temperature Measurements Using Raman Lidar. NASA TN D-7679, 1974.

2. Salzman, J. A.; and Coney, T. A.: Remote Measurement of Atmospheric Temperatures by Raman Lidar. NASA TN X-68250, 1973.

3. Coney, T. A.; and Salzman, J. A.: Determination of the Temperature of Gas Mixtures by Using Laser Raman Scattering. NASA TN D-7126, 1973.

4. Cooney, J.: Measurement of Atmospheric Temperature Profiles by Raman Backscatter. J. App. Meteor., Vol. 11, 1972, pp. 108-112.

5. Strauch, J. C.; Derr, V.; and Culp, R. E.: Atmospheric Temperature Measurement Using Raman Backscatter. App. Optics, Vol. 10, 1971, pp. 2665-2669.

6. Grossman, J. J.: Filter Spectrograph. U. S. Patent 3,865,490, Feb. 11, 1975.

APPENDIX A

Recommended LeRC System Modifications

Remote temperature measurement of gases using rotational Raman spectroscopy has been considered by a number of investigators. Salzman and Coney (References 1 and 2) found that only the anti-Stokes spectrum can be used to measure temperature unless stray laser radiation and luminescence background (aerosol) in the Stokes spectrum is independently measured and subtracted. They also pointed out that by taking ratios of rotational spectrum line pairs (line intensities measured simultaneously) high temporal resolution (range resolved profiling) is attained, the frequency bandwidth becomes small minimizing(making negligible) atmospheric transmission path differences, and finally that sensitivity can be gained by using sums of selected line combinations.

Formally, the Stokes and anti-Stokes line intensities for rotational level J are

$$I_J(s) = C \frac{(J+1)(J+2)}{(2J+3)} \frac{\Theta}{T} \exp\left[- J (J+1) \frac{\Theta}{T} \right]$$

$$I_J(as) = C \cdot \frac{J(J-1)}{(2J-1)} \frac{\Theta}{T} \exp\left[- J (J+1) \frac{\Theta}{T} \right] \qquad \text{(A-1)}$$

or

$$I_J(s) = C\, S_J(s) \frac{\Theta}{T} \exp\left[- R_J \frac{\Theta}{T} \right]$$

$$I_J(as) = C\, S_J(as) \frac{\Theta}{T} \exp\left[- R_J \frac{\Theta}{T} \right] \qquad \text{(A-2)}$$

Three temperatures can be defined for line pairs where J and K are quantum numbers for two different rotational transitions. In each case, the objective is to eliminate the preexponential $C\Theta/T$ so that the exponential dependence is the only one left. These three temperatures are

a. Stokes Temperature

For a line pair intensity ratio

$$\frac{1}{T} = \frac{\ln [I_J(s)/I_K(s)] - \ln [S_J(s)/S_K(s)]}{(R_K - R_J)\,\Theta} \tag{A-3}$$

and for a line pair difference and sum

$$\frac{1}{T} = \frac{\ln [(I - \Delta I)/(I + \Delta I)] - \ln [S_J(s)/S_K(s)]}{(R_K - R_J)\,\Theta} \tag{A-4}$$

where

$$I = I_K + I_J$$

$$\Delta I = I_K - I_J$$

The above equations are identical for a given line pair. For multi-line operation, sums and differences of intensities are the natural observables and for this case Equations (A-3) and (A-4) are not equivalent.

b. Anti-Stokes Temperatures

The equations corresponding to (A-3) and (A-4) above are

$$\frac{I}{T} = \frac{\ln[I_J(as)/I_K(as)] - \ln [S_J(as)/S_K(as)]}{(R_K - R_J)\,\Theta} \tag{A-5}$$

and

$$\frac{1}{T} = \frac{\ln [(I - \Delta I)/(I + \Delta I)] - \ln [S_J(as)/S_K(as)]}{(R_K - R_J)\,\Theta} \tag{A-6}$$

c. Combination Stokes and Anti-Stokes Temperature

The ratios of individual Stokes and anti-Stokes lines for constant J are constant, independent of temperature.

$$\frac{I_J(s) - I_J(as)}{I_J(s) + I_J(as)} = \frac{S_J(s) - S_J(as)}{S_J(s) + S_J(as)} \tag{A-7}$$

However, if the sums and differences are taken of the complete Stokes and anti-Stokes bands, the preexponential $C\Theta/T$ drops out and the temperature dependence appears in the infinite series of sums and difference terms.

$$\frac{I(s) - I(as)}{I(s) + I(as)} = \frac{\Sigma_J^{\infty} [S_J(s) - S_J(as)] \exp [-R_J \Theta/T]}{\Sigma_J^{\infty} [S_J(s) + S_J(as)] \exp [-R_J \Theta/T]} \qquad \text{(A-8)}$$

or explicitly

$$\frac{\Delta I(\cdot)}{\Sigma I(\cdot)} = \frac{\Sigma_J^{\infty} \left(\frac{2J^2 + 2J - 1}{2J^2 + 2J - 3} \right) \exp \left(-J(J + 1) \Theta/T \right)}{\Sigma_J^{\infty} \left(\frac{4J^3 + 6J^2 - 2J - 2}{4J^2 + 4J - 3} \right) \exp \left(-J(J + 1) \Theta/T \right)} \cdot \qquad \text{(A-9)}$$

This intensity ratio, which can be approximated by

$$\frac{\Delta I(\cdot)}{\Sigma I(\cdot)} = \frac{\Sigma_J^{\infty} \exp [-J(J + 1) \Theta/T]}{\Sigma_J^{\infty} \frac{2J^2}{(2J-1)} \exp [-J(J + 1) \Theta/T]} , \qquad \text{(A-10)}$$

is a universal function of Θ/T. When Θ is known a temperature T is uniquely determined by $\Delta I(\cdot)/\Sigma I(\cdot)$. This is not true for Stokes and anti-Stokes temperatures when band segmentation and summation is used to improve the experimental accuracy. Some knowledge of the measurement system must be used to determine the empirical correction factor related to imperfect band segmentation.

If the Stokes measurement is possible the best temperature resolution is probably obtained by using both the Stokes and anti-Stokes band intensities. To some extent this advantage may be offset by the loss of an analytic explicit functional relationship between the temperature and the intensities, Equations (A-4) and (A-6). Nevertheless, numerical solutions are available, and experimentally measured temperatures and errors can be used to verify the theoretical computation of integrated intensities over all J values (prescription: use generalized equations (A-4), (A-6), and (A-8)).

The MDAC system has been shown to provide both adequate laser line rejection (a factor greater than 10^{11}) to eliminate instrumental and aerosol scattering noise signals, and adequate spectral resolution to measure and subtract aerosol fluorescence background noise. In addition, both the spectral and background bands can be divided instrumentally to give the

desired sum and difference signals in forms directly usable for analog or digital computation of the measured temperature.

Salzman and Coney have reported experimental verification that temperatures can be measured to within ±3°K using the ratios of two anti-Stokes band measurements. Both of the bands are selected by narrow band dielectric filters, one centered at the rotation band maximum ($\Delta\nu$ = 50 cm^{-1}, a point where the temperature coefficient is approximately zero over the temperature range −25°C to +15°C) and the second 2.6 nm wide containing some 12 rotational lines of O_2 and N_2. Since it is beyond the state of the art today to manufacture dielectric interference filters which will eliminate the laser line at center wavelengths closer than 40 cm^{-1}, the first portion of the rotation bands (namely J = 1 to J ≅ 8) cannot be used. Unfortunately, this portion contains about half of the total ΔT information. Their wide band filter (2.6 nm) collects 33% of the energy and the narrow band filter about 14%. If all the energy could be used the ΔT would be improved by a factor greater than 3.4. This conservative estimate includes the $\sqrt{2}$ factor from the sum of both the Stokes and anti-Stokes bands.

A remote sensing system with improved signal to noise characteristics provides increased temperature accuracy, extended range at the same accuracy, or some combination of both. Since the MDAC Laser Line Filter System can be identified as a combination of a spectrograph and a laser line filter, a number of new options are available where the laser line filter section alone is used in combination with different band selective filters. Dielectric filters such as those used by Salzman and Coney can be used. The narrow band filter is widened to be as close to the laser line (20 cm^{-1}) as possible. The dielectric filter attenuation (10^{-3}) and the LLF section attenuation (10^{-7}) satisfy the design goal of 10^{-10} total laser light attenuation with adequate separation between extended Raman bands. Two additional dielectric filter channels can be added easily to measure the Stokes bands since the laser line itself is taken out and can be measured at the LLFM assembly. However, to do this a slightly different LLFM must be developed and fabricated. It has to reject the laser line over the entire aperture, and transmit only the background signal over half the aperture. Then the measured fluorescent background can be subtracted from the Stokes band signals, which can now be used to calculate the Stokes temperature. Although it is conceptually easy to

design and fabricate this modified LLFM assembly, it requires interfacing a number of fabrication technologies which would make fabrication an independent but parallel development program.

Another choice is the combination of dielectric and Fabry-Perot filters. The Fabry-Perot, when set for transmitting only the rotation band lines, rejects the laser line. Therefore, for a pure gas the Stokes temperature could be measured using two etalons and two dielectric filters. The first etalon rejects the laser line and the first dielectric filter rejects the anti-Stokes band. The second etalon transmits the rotation lines and reflects the fluorescence signal which is measured. The transmitted rotation lines are separated by a second dichroic dielectric filter into both the longer wavelength and shorter wavelength Stokes lines. The signals can be combined electrically during measurement or by computer if the three detector signals are recorded in parallel. Alternatively the LLF and one etalon can be used with three detectors.

Although there is a potential cost saving in using dielectric filters when measuring only the anti-Stokes band, combinations of filters for Stokes band measurements using Fabry-Perot filters can be equally as complex as a grating spectrograph output filter in the LLFS. An output aperture (A, Figure 2) should be included in the LLFS for viewing the filter section output directly. Then other filter configurations and combinations can be tested. This would be important for testing those applications in which weight and volume play important factors.

The recommended rotational Raman remote temperature measuring system should be designed as follows:

a. Use existing input optics and photodetector equipment where possible.

b. Change the present configuration as follows (See Figure 2): direct the input beam through a new slit to impinge directly on the collimating mirror along a path parallel to GJ and have the LLF output selectably pass through either the present intermediate slit using diagonal mirror G or output through the presently used input slit L by retractable mirror K. This creates a set of one input and two exit beam paths which are mutually perpendicular. The LLF output can be used for interference filter measurements by mating the system with the existing LeRC anti-Stokes dielectric filter system.

c. Use separate mirrors for the input collimating mirror and the output focusing mirror.

d. Build a new housing so that there is easy access to all optical components.

e. Use a grating drive system if more than one laser line is to be selected, or a simple coarse and fine setting system for single laser frequency operation.

APPENDIX B

Symbols

c	Velocity of light, 3×10^{-8} m sec^{-1}.
C	Constant in equation for Raman scattering intensities.
$C(\lambda_L;\lambda_{as})$	Wavelength drive counter reading for the laser line exiting the LLFM slit when PMT measuring an anti-Stokes line intensity.
$C(\lambda_s;\lambda_L)$	Wavelength drive counter reading for the anti-Stokes line exiting the LLFM slit when PMT measuring the laser line intensity.
I	$= I_k + I_J$, amps.
ΔI	$= I_K - I_J$, amps.
$\Delta I(\cdot)$	= I(s) - I(as), amps.
$\Sigma I(\cdot)$	= I(s) + I(as), amps.
$I(\lambda;\lambda)$	Signal intensity measured at wavelength λ, amps.
$I(\lambda_i;\lambda)$	Measured light intensity of wavelength λ_i, when filter is set to measure wavelength λ, amps.
$I(\lambda_L;\lambda)$	Laser light noise signal when measuring signal at wavelength λ, amps.
$I(\lambda_L;\lambda_L)$	Laser light intensity measured at wavelength λ_L, amps.
I(as)	Complete anti-Stokes rotational Raman band intensity, amps.
I(s)	Complete Stokes rotational Raman band intensity, amps.
$I_J(as)$	Anti-Stokes Raman line intensity for rotational energy level J, amps.
$I_J(s)$	Stokes Raman line intensity for rotational energy level J, amps.
J	Rotational state quantum number.
K	Rotational state quantum number.
R	= J(J+1) .

S/N	Signal to noise ratio.
$S_J(as)$	= J(J-1/(2J-1).
$S_J(s)$	= (J+1)(J+2)/(2J+3).
T	Temperature, °K.
ΔT	Temperature change, °K.
θ	Rotational characteristic temperature, °K.
λ	Wavelength, nm.
λ_{as}	Anti-Stokes Raman wavelength, nm.
λ_L	Laser wavelength, nm.
λ_s	Stokes Raman wavelength, nm.
$\rho(L)$	Laser line rejection efficiency.
$\tau(L)$	Laser line attenuation ratio or transmission efficiency.

Distribution List - Final Report NAS3-17818

NAME	NO. OF COPIES
NASA Scientific and Technical Information Facility Box 33 College Park, MD 20740 Attn: NASA Representative	2
National Technical Information Service Springfield, VA 22151	20
NASA Lewis Research Center 21000 Brookpark Road Cleveland, OH 44135 Attn: Jack A. Salzman Mail Stop 301-1	5
NASA Headquarters Washington, DC 20546 Attn: J. A. Suddreth Mail Code RLN	1
AVCO Everett Research Laboratory 2385 Revere Beach Parkway Everett, MA 02149 Attn: D. A. Leonard	1
Drexel University Physics Department Philadelphia, PA 19104 Attn: Dr. John Cooney	1
General Electric Company Corporate Research and Development P. O. Box 8 Schenectady, NY 12301 Attn: Dr. D. R. White	1
Polytechnic Institute of Brooklyn 333 Jay Street Brooklyn, NY 11201 Attn: Dr. S. Lederman	1

NAME	NO. OF COPIES
Purdue University Project Squid School of Mechanical Engineering Lafayette, IN 47907 Attn: Dr. R. Goulard	1
NASA Lewis Research Center 21000 Brookpark Road Cleveland, OH 44135 Attn: Contract Section B Mail Stop 500-313	1
Technical Report Control Office Mail Stop 5-5	1
Technology Utilization Office Mail Stop 3-19	1
AFSC Liason Office Mail Stop 501-3	1
Office of Reliability & Quality Assurance Mail Stop 500-211	1
Library Mail Stop 60-3	2
Patent Counsel Mail Stop 500-113	1